Using ab Initio MO Calculations To Understand the Photodissociation Dynamics of CH_2CCH_2 and CH_2C_2

W. M. Jackson,*,†,‡ A. M. Mebel,† S. H. Lin,*,†,§,|| and Y. T. Lee†,⊥

Institute of Atomic and Molecular Sciences, Academia Sinica, P.O. Box 23-166, Taipei 10764, Taiwan, ROC, Department of Chemistry, University of California, Davis, California 95616, Department of Chemistry, National Taiwan University, Taipei 106, Taiwan, ROC, Department of Chemistry and Biochemistry, Arizona State University, Tempe, Arizona 85284-1604, and Department of Chemistry, University of California, Berkeley, California 94720

Received: February 17, 1997; In Final Form: April 18, 1997[⊗]

Potential energy surfaces (PES) of the ground and excited states of allene C_3H_4 and vinylidenecarbene C_3H_2 have been studied by *ab initio* CCSD(T) and MRCI methods. The three lowest singlet excited states of allene, $^1A_2$, $^1B_1$, and ^1E, are calculated to have the vertical excitation energies of 6.10, 6.55, and 6.94 eV, respectively. Three local minima are found on the excited S_1 surface, **2b** (^1A_g, D_{2h}), **5** ($^1A''$, C_s), and **10** ($^1B_2$, C_{2v}'), and their adiabatic excitation energies are 3.02, 3.05, and 4.70 eV, respectively. The PES of the ground and excited states are shown to cross when the geometry of allene changes by twisting the CH_2 groups and bending the CCC angle or along the pathway that leads to H_2 detachment. For vinylidenecarbene the lowest singlet excited states are $^1A_2$ and $^1B_1$ with the respective vertical excitation energies of 1.88 and 2.44 eV and the adiabatic excitation energies of 1.77 and 2.05 eV. The endothermicity of the $C_3H_4 \rightarrow C_3H_2 + H_2$ reaction is predicted to be ∼83 kcal/mol with the barrier of ∼92 kcal/mol on the S_0 surface. The calculations suggest the most likely mechanism for photodissociation of allene at 193 nm to produce $C_3H_2 + H_2$ involves a Franck−Condon transition to the $^1B_1$ excited state. This is followed by a twisting of the CH_2 groups and then conversion to the vibrationally excited ground state through the seam of crossing. Once the vibrationally excited allene molecule is in the ground electronic state it dissociates to produce $C_3H_2 + H_2$.

Introduction

Recent experimental studies on the photodissociation of allene showed that one of the photodissociation channels produces C_3H_2 and H_2.[1−3] The C_3H_2 molecules undergo secondary photolysis to produce C_3 by molecular detachment of H_2. It has been suggested that such a process can lead to the formation of the C_3 molecules in comets.[3] The C_3H_2 molecule is also one of the simplest diene species that is thought to be a precursor for the formation of soot in flames[4] and one of the reactants that could lead to unsaturated molecules in the interstellar medium.[5−7]

The laser induced fluorescence (LIF) study of the photodissociation of allene[2] at 193 nm showed that when C_3H_2 was photodissociated it produced C_3 with very cold rotational distributions in the 000 and 010 states. A geometrical isomer of allene, propyne, has a geometry and electronic structure that is distinctly different. It also absorbs at 193 nm and it was postulated that dissociation of this species should lead to a C_3 fragment with a rotational distribution which is distinctly different from the one observed from allene. In fact, what was observed is a rotational population identical to the one observed from allene. These LIF results[2] were explained by using the following reaction scheme:

$$CH_2CCH_2\ (X\ ^1A_1) + h\nu_{193\ nm} \rightarrow CH_2CCH_2\ (^1B_1) \quad (1)$$

$$CH_2CCH_2\ (^1B_1) \rightarrow CH_2CCH_2^{\ddagger}\ (X\ ^1A_1) \quad (2)$$

$$CH_2CCH_2^{\ddagger}\ (X\ ^1A_1) \rightarrow H_2C_3 + H_2 \quad (3)$$

$$CH_3CCH\ (X\ ^1A') + h\nu_{193\ nm} \rightarrow CH_3CCH^* \quad (4)$$

$$CH_3CCH^* \rightarrow CH_3CCH^{\ddagger}\ (X\ ^1A') \quad (5)$$

$$CH_3CCH^{\ddagger}\ (X\ ^1A') \rightarrow H_2C_3 + H_2 \quad (6)$$

$$H_2C_3 + h\nu_{193\ nm} \rightarrow C_3\ (X\ ^1\Sigma^+_g) + H_2 \quad (7)$$

The initial photoexcitation of allene and propyne puts them in different Franck−Condon regions on their respective excited states. Direct dissociation from the different Franck−Condon regions on these excited states would lead to C_3H_2 products with different internal energies. This in turn should give C_3 radicals with different internal energies, which is contrary to the observations. To obtain identical rotational distributions for the observed C_3, one is forced to postulate that the intermediate that is photolyzed in reaction 7 has to be the same for both allene and propyne. One obvious way to do this is the conversion of electronically excited allene and propyne to the vibrationally excited C_3H_4 on the ground state surface via reactions 2 and 5 before dissociation occurs. Once it is on this surface theoretical calculations[8−11] show that a C_3H_4 molecule with internal energy of 148 kcal/mol is above all barriers to 1,2- and 1,3-H atom migration, as well as all other barriers to

† Academia Sinica.
‡ University of California, Davis.
§ National Taiwan University.
|| Arizona State University.
⊥ University of California, Berkeley.
⊗ Abstract published in *Advance ACS Abstracts,* July 1, 1997.

S1089-5639(97)00597-5 CCC: $14.00

isomerization. So it is conceivable that once the molecule is on this surface, the same intermediate can be formed by hydrogen migration before dissociation. On the other hand, the equilibration may happen after the H_2 detachment from allene or propyne if C_3H_2 formed in reactions 3 and 6 have enough internal energy for isomerization.

In order to understand the mechanism and dynamics of the photodissociation of allene and propyne leading eventually to C_3, one has to study potential energy surfaces (PES) of various isomers of C_3H_4 and C_3H_2, their isomerization, and H_2 elimination in the ground and excited states which are accessible with absorption of a 193 nm photon. In the present paper, we consider the electronic spectrum of allene (reaction 1) and PES for excited states of allene in order to clarify how reaction 2 can take place. We analyze the potential energy surface for H_2 elimination from allene, reaction 3. Ground and excited state PES's of one of the isomers of C_3H_2, vinylidenecarbene, formed by the H_2 detachment from allene are also considered.

Methods of Calculations

For the ground electronic state, the geometries of C_3H_4, C_3H_2, and transition states for H_2 detachment have been optimized by using the hybrid density functional B3LYP method[12] with the 6-311G(d,p) basis set.[13] Vibrational frequencies, calculated at the B3LYP/6-311G(d,p) level, have been used for characterization of the stationary points and zero-point energy (ZPE) correction. In order to obtain more accurate energies on the ground state PES we used the CCSD(T) approach[14] with the large 6-311+G(3df,2p) basis set. The CCSD(T)/6-311+G(3df,2p)//B3LYP calculational scheme has been shown[15] to provide accuracies of 1−2 kcal/mol for the atomization energies of the G2 test set of molecules. A similar approach has also been demonstrated to be accurate for transition state energies.[16] In some cases, for comparison, we additionally carried out the CCSD(T) calculations with Dunning's correlation consistent cc-pVTZ basis set.[17]

For excited states, geometry optimization of various stationary points has been carried out by using the multireference CASSCF method[18] with the 6-311+G(d,p) basis set. For C_3H_4 the active space included four electrons distributed on six orbitals, CASSCF(4,6). For the D_{2d} symmetric structure of allene the active space consisted of the electrons forming two CC bonds of π-type on $2b_1+2b_2+2a_1$ orbitals (in terms of C_{2v} subgroup). For the planar C_{2v} and C_s allenic species the active space included $3a_1+1b_1+1b_2+1a_2$ and $4a'+2a''$ orbitals, respectively. In the cases when the energies of two electronic states are close to each other, particularly for the search of a minimum on the S_1 surface of allene and of crossing points for the S_1 and S_0 surfaces, we used state-averaged (s/a)-CASSCF[19] calculations with equal weights for both states and with a larger active space, eight electrons on 10 orbitals. The search of the crossing points has been performed by minimizing the energy difference between two states at the s/a-CASSCF(8,10)/6-311+G(d,p) level. For optimization of the geometries of vinylidenecarbene, we used the active space including six electrons, four π electrons and two electrons forming a lone pair on the hydrogen-less carbon atom, distributed on nine orbitals, $3a_1+3b_1+3b_2$. In some cases, the frequency calculations for excited states of C_3H_2 have been carried out at the simpler CIS/6-311+G(d,p) level.[20]

The energies of excited state structures were refined by using internally contracted MRCI calculations.[21] The CASSCF optimized geometries were used in the MRCI calculations assuming that the shapes of potential energy surfaces are similar at both levels of theory. The MRCI minima or saddle points may slightly deviate from those optimized at CASSCF, however, the MRCI geometry optimization for the molecules of this size is at present prohibitly expensive. Both for C_3H_4 and C_3H_2 the CASSCF(8,10) wavefunction was used as a reference for the MRCI(4,8) computation with the Davidson correction for quadruple excitations. The basis set used in the MRCI calculations is ANO(2+), i.e., the ANO basis set[22] (4s3p2d for C, 3s2p for H) augmented with several diffuse functions for the carbon atom (s exponents, 0.012 138 and 0.004 224 82; p exponents, 0.008 015 0 and 0.002 805 2; d exponent: 0.028 512).[23] The ANO(2+) basis set has been tested for the calculations of the valence and Rydberg excited state energies of various hydrocarbons and shown to provide a high accuracy.[23] For comparison, we have also carried out the equation-of-motion coupled cluster (EOM-CCSD)[24] calculations with the 6-311-(2+)G** basis set[25] for the vertical excitation energies of allene and vinylidenecarbene.

The MOLPRO-96,[26] GAUSSIAN 94,[27] and ACES-II[28] programs were used for the calculations.

Results and Discussion

Excited Electronic States of Allene. The absorption spectrum of allene is rather complex.[29−32] It is generally agreed that the weak, featureless absorption below 6.45 eV is due to the forbidden $^1A_1$ (S_0) → $^1A_2$ (S_1) transition and the intense, structured band between 8.5 and 9.0 eV is due to the allowed $^1A_1 \rightarrow {}^1B_2$ vertical excitation. Four distinct absorption bands are observed between 6.54 and 9 eV, including a weak band with a maximum at 6.70 eV, a strong broad absorption covering the 6.95−7.85 eV range, and two bands in the 8.02−8.38 and 8.5−9.0 eV ranges. There have been a number of theoretical studies of vertical excitation energies for allene, including perturbative configuration interaction (CI) calculations of Rauk et al.,[33] CI calculations of Diamond and Segal,[34] and equation-of-motion calculations of Galasso and Fronzoni.[35] Their results and the results of the present calculations are summarized in Table 1.

The first two excited states of allene are $^1A_2$ (6.10 eV at our best MRCI+D level) and $^1B_1$ (6.55 eV), corresponding to the $\pi \rightarrow \pi^*$ transitions. In the ground state, allene has the following valence electronic configuration, $1a_1^2 1b_2^2 2a_1^2 2b_2^2 1e^4 2e^4$. Transitions of one electron from 2e to 3e have $\pi \rightarrow \pi^*$ character and produce four excited states of A_2, B_1, B_2, and A_1 symmetry. Both $^1A_1 \rightarrow {}^1A_2$ and $^1A_1 \rightarrow {}^1B_1$ transitions are symmetry-forbidden and have zero oscillator strength. The first allowed transition is $\pi \rightarrow 3s$, to the ^1E Rydberg state. ^1E has the vertical excitation energy of 6.94 eV and the oscillator strength of 0.04. The next $^1A_1 \rightarrow {}^1B_2$ ($\pi \rightarrow \pi^*$) transition has a large oscillator strength of 0.24 at the MRCI level, and the vertical excitation energy, 7.65 eV, is significantly higher than the energy of a 193-nm photon, 6.42 eV. We will return to the question which state is most likely to absorb the 193-nm photons later, after considering the optimized geometries for the excited states and adiabatic excitation energies.

PES of the allene ground state is well studied.[36−39] Most of earlier calculations concern with the transition state (TS) for the internal rotation. At various levels of theory the calculated barrier is in the 45−50 kcal/mol range, in agreement with experimental barriers for substituted derivatives of allene (46−47 kcal/mol).[40] The TS (structure **3** in Figure 1) is a planar bent C_{2v} symmetric species corresponding to $^1A_2$ singlet biradical.

Figure 2a illustrates the behavior of the ground and four lowest lying singlet excited states of allene upon the CH_2 twisting when the linearity of CCC is maintained. The ground state $^1A_1$ (D_{2d}) correlates with ^1A (D_2) and ^1A_u (D_{2h}), so the

TABLE 1: Vertical Excitation Energies (eV) for Allene, Calculated at Various Levels of Theory

state	character	CASSCF(8,10) /ANO(2+)	MRCI(4,8) /ANO(2+)	MRCI+D /ANO(2+)	osc str.	EOM-CCSD /6-311(2+)G**	osc str	CI[a]	CI[a]	EOM[c]
$^1A_2$	$\pi \rightarrow \pi^*$	5.89	6.19	6.10	0	6.23	0	6.49	6.57	6.86
$^1B_1$	$\pi \rightarrow \pi^*$	6.55	6.70	6.55	0	6.65	0	6.84	6.92	7.23
^1E	$\pi \rightarrow 3s$	5.84	6.85	6.94	0.037	7.02	0.030	7.21	6.87	7.73
$^1B_2$	$\pi \rightarrow \pi^*$	7.13	7.55	7.56	0.236	7.62	0.411	7.88	7.45	8.03
2^1A_1	$\pi \rightarrow 3p/\pi \rightarrow \pi^*$					7.69	0	8.15−8.25	7.61	8.28
2^1E	$\pi \rightarrow 3p$					7.82	0.017	8.13	7.69	8.54
2^1A_2	$\pi \rightarrow 3p$					8.05	0	8.25	7.82	9.01
2^1B_1	$\pi \rightarrow 3p$					8.06	0	8.15−8.25	7.85	9.02
3^1A_1	$\pi \rightarrow 3d/\pi \rightarrow \pi^*$					8.27	0	8.56	8.31	9.19
3^1E	$\pi \rightarrow 3d$					8.46	0.019	8.72	8.20	9.24
2^1B_2	$\pi \rightarrow 3d$					8.61	0.083	8.86	8.34	9.73
4^1E	$\pi \rightarrow 3d$					9.25	0.013	8.91−8.95	8.42	

[a] From ref 33. [b] From ref 34. [c] From ref 35.

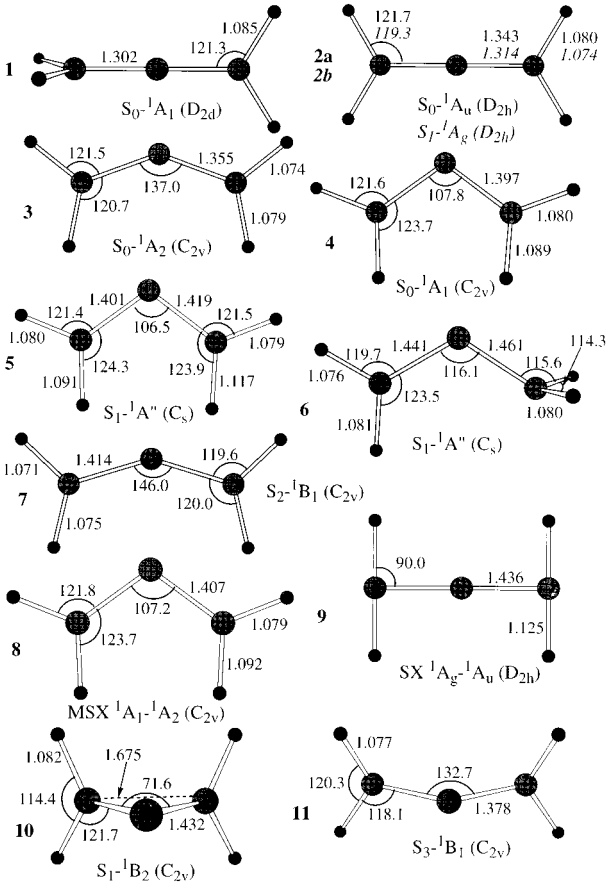

Figure 1. CASSCF/6-311+G** optimized geometries of various structures of allene in the ground and excited singlet electronic states.

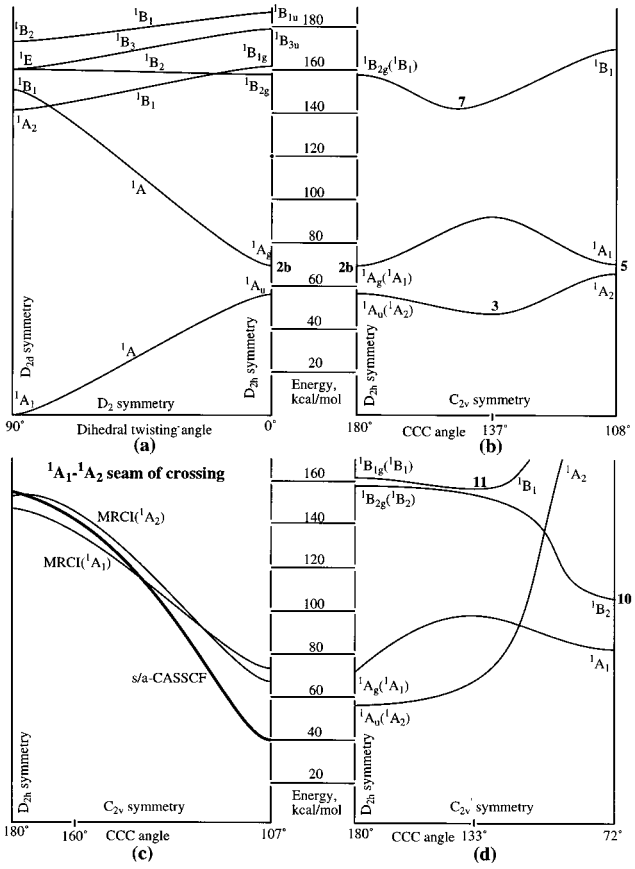

Figure 2. (a) PES of the ground and excited states of allene as functions of the dihedral CH_2 twisting angle. (b) PES of the $^1A_1$, $^1A_2$, and $^1B_1$ states within C_{2v} symmetry as functions of the CCC angle; (c) approximate $^1A_1-^1A_2$ seam of crossing within C_{2v} symmetry as a function of the CCC angle; (d) PES of the $^1A_1$, $^1A_2$, $^1B_2$, and $^1B_1$ states within C_{2v}' symmetry as functions of the CCC angle. Bold numbers show the location on PES's of the various equilibrium structures, presented in Figure 1.

wavefunction changes its character from a closed shell singlet to an open shell singlet. At the planar D_{2h} symmetric geometry the open shell ^1A_u state (structure **2a**) lies 13.2 kcal/mol lower than the closed shell ^1A_g (structure **2b**). The first excited state $^1A_2$ (D_{2d}) correlates with $^1B_1$ (D_2) and $^1B_{1g}$ (D_{2h}) and its energy increases from 140.7 kcal/mol at the ground state geometry to 161.8 kcal/mol at the D_{2h} geometry. On the contrary, the energy of the second excited state $^1B_1$ (D_{2d}), correlating with 2^1A (D_2) and ^1A_g (D_{2h}), rapidly goes down. As was discussed in detail by other authors,[37,41] the $^1B_1$ (D_{2d}) state is stabilized by D_2 torsion according to Walsh's rules.[42] The doubly occupied 2e and virtual 3e* MO's in D_{2d} symmetry split into in-plane σ and out-of-plane π components, with the energies and symmetries such that $b_{3u}(\pi) < b_{2g}(\pi) < b_{2u}(\sigma^*) < b_{3u}(\pi^*)$ for the $D_{2d} \rightarrow D_2 \rightarrow D_{2h}$ transformation. On the basis of Walsh's rules, the σ^* A_u ($b_{2g}(\pi) \times b_{2u}(\sigma^*)$) is the stabilized form of the B_1 Franck−Condon state. However, because B_1 collapses to the totally symmetric representation (A) at intermediate D_2 geometries, the ground state (1^1A_1) ultimately correlates with the open shell ^1A_u and the excited $^1B_1$ state with the closed shell excited state $(1b_{3u})^2(1b_{2g})^2$ ^1A_g. The ^1E state splits into $^1B_2$ and $^1B_3$ within D_2 symmetry. The energy of $^1B_2$ slightly decreases, from 160.0 kcal/mol for ^1E (D_{2d}) to 158.9 kcal/mol for $^1B_{2g}$ (D_{2h}), while the energy of the $^1B_3$ component increases. The fourth excited state is $^1B_2$ (D_{2d}) corresponding to $^1B_1$ (D_2) and $^1B_{1u}$ (D_{2h}), and its energy also increases. The $^1B_1$ and 2^1A as well as the $^1B_1$ and $^1B_2$ surfaces have to cross within D_2 symmetry.

The D_{2h} symmetric structure **2b** apparently is a local minimum on the PES of the first excited singlet state. The

B3LYP calculations of Bettinger et al.[39] gave no imaginary frequencies for this structure, while the CASSCF(4,6) calculations give one imaginary frequencies for **2b**. More accurate s/a-CASSCF(8,10) optimization without symmetry constraints starting from geometries with ∠CCC ≥ 140° converges to **2b**, confirming that it is a local minimum. Another local minimum on S_1, also optimized without any symmetry constraints by s/a-CASSCF(8,10), is a planar structure **5** with ∠CCC = 106.5°. Geometry of **5** is close to that of **4** ($^1A_1$,C_{2v}) which has one imaginary frequency and corresponds to a transition state on the S_0 surface. The adiabatic excitation energies for **2b** (^1A_g, D_{2h}) and **5** ($^1A''$, C_s) are close, about 70 kcal/mol at the MRCI+D level. Another stationary point located on the S_1 surface, nonplanar structure **6** ($^1A''$, C_s), is a transition state for the rotation of one of the CH_2 fragments.

The S_0 and S_1 surfaces cross when the CCC fragment bends within C_{2v} symmetry. We found two points on the seam of crossing, **8** (C_{2v}) and **9** (D_{2h}), with the energies of 66.1−72.5 and 147.4−154.5 kcal/mol, respectively. Interestingly, the geometry of **8**, which is likely to be the minimum on the seam of crossing (MSX), is similar to those of **4** and **5**. The transition state on S_0 (**4**), the minimum on S_1 (**5**) and MSX **8** lie in close vicinity of each other. Figure 2c shows the profile of the $^1A_1$−$^1A_2$ seam of crossing along the CCC angle at the planar C_{2v} geometry. At ∠CCC = 160° the crossing occurs in the 135−143 kcal/mol energy range. A crossing point with the energy of a 193 nm photon has the CCC angle between 160° and 180°.

The minimum on S_2 surface is **7** ($^1B_1$, C_{2v}). The geometry of **7**, is similar to that of **3**, but with longer CC distances (1.41 Å) and a larger CCC angle (146°). The relative energy of **7** with respect to **1**, i.e., the adiabatic excitation energy for the second excited state, is 147.3 kcal/mol. We located also two minima within nonplanar C_{2v}' symmetry with the C_2 axis perpendicular to the molecular plane in D_{2h}. Structure **10** ($^1B_2$) has a three-member CCC cycle and its geometry is close to that of the triplet cyclopropylidene. The ring closure on the $^1B_2$ surface occurs without barrier. $^1B_2$ is the lowest excited singlet state at the geometry of **10**. The adiabatic excitation energy, **1** → **10**, is 108.3 kcal/mol. **11** ($^1B_1$, C_{2v}') is a minimum on the S_3 and its adiabatic excitation energy is 158.6 kcal/mol.

The results of our calculations illustrated in Figures 2a−d show that the potential energy surfaces of the ground and several excited states of allene cross when geometry of the molecule changes by twisting the CH_2 groups and bending the CCC angle. As compared to the ground state, the geometry changes in the excited states are very large and the adiabatic excitation energies in the cases of structures **2b**, **5**, and **10** are much lower than the vertical excitation energies. Therefore, one can expect that the vibronic spectra of allene corresponding to the $^1A_2$, $^1B_1$, and ^1E states have numerous weak peaks with very low Franck−Condon factors spread over a broad energy region. The spectra would be similar to the vibronic spectrum of ethylene due to the $\pi \rightarrow \pi^*$ ($^1A_g \rightarrow {}^1B_{1u}$) transition.[32,43] Correspondence between the vertical and adiabatic excited states is complicated. Within the symmetry consideration, discussed above, vertical $^1B_1$ (D_{2d}) correlates with **2b** and **5**, ^1E correlates with **7** (C_{2v}, $^1B_1$) and **10** (C_{2v}', $^1B_2$), and $^1A_2$ correlates with **11**. However, if the symmetry constraints are lifted and all surface crossings are considered as avoided crossings, $^1A_2$ should correlate with **2b**, **5**, and **10**, $^1B_1$ should correlate with **7**, and ^1E should correlate with **11**.

Although the $^1A_1 \rightarrow {}^1A_2$ and $^1A_1 \rightarrow {}^1B_1$ transitions are symmetry forbidden, the $^1A_2$ and $^1B_1$ states could absorb light due to vibronic coupling. The $^1B_1$ state is most likely to absorb the 193 nm photons according to the calculated energetics. One may not exclude also some absorption by the ^1E state. The vertical excitation energy of this state, 160.0 kcal/mol, is significantly higher than $h\nu_{193\ nm}$, but the adiabatic excitation energy may be considered as low as 108.3 kcal/mol for **10**. In general, the results indicate that the absorption cross section at this wavelength should be very low, which agrees with the experimental observations.[1] For the photodissociation dynamics, we expect that it is not critical which excited state of allene, $^1A_2$, $^1B_1$, or ^1E, is formed after the absorption of a photon. The lifetime of these states is expected to be short because of the possibility of fast transformation into vibrationally excited ground electronic state by internal conversion or by hopping from one potential energy surface to another via the respective seam of crossing. For the $^1E \rightarrow {}^1B_1$ and $^1B_1 \rightarrow {}^1A_2$ transitions, the internal conversion mechanism can be preferable because the vibronic coupling between these state is nonzero in the first order approximation and the energy gap between them is small. On the other hand, for the $^1B_1 \rightarrow {}^1A_1$ or $^1A_2 \rightarrow {}^1A_1$ transitions the surface hopping mechanism seems to be favorable. The internal conversion would be slow because of two factors, zero first-order vibronic coupling due to the fact that the transitions are symmetry-forbidden and the large energy gap at the ground state geometry.

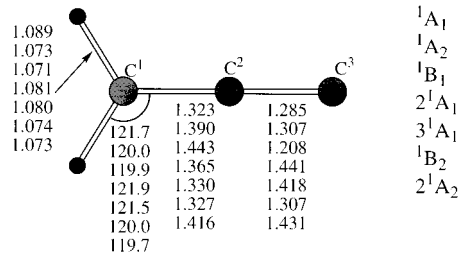

Figure 3. CASSCF(6,9)/6-311+G** optimized geometries of vinylidenecarbene in the ground and excited electronic states within C_{2v} symmetry.

Excited Electronic States of Vinylidenecarbene. In this section we consider vertical excitation energies, optimized geometries and adiabatic excitation energies for one of the isomers of C_3H_2, vinylidenecarbene, which is formed after H_2 detachment from allene. The geometries are shown in Figure 3 and the excitation energies are presented in Table 3. The wavefunction of vinylidenecarbene has the following configuration, $1a_1^2 2a_1^2 3a_1^2 4a_1^2 5a_1^2 6a_1^2 1b_2^2 1b_1^2 7a_1^2 2b_2^2$. Here, orbitals $1b_1$ and $2b_2$ correspond to the CC bonds of π-type. $1b_1$ (π) is perpendicular to the molecular plane and $2b_2$ (π') lies in the plane and connects the central C^2 and the bare C^3 carbon atoms. $7a_1$ contains the lone pair of C^3.

The first excited state of C_3H_2 is $^1A_2$, which has the $\pi' \rightarrow \pi^*$ character and the $1b_1^2 7a_1^2 2b_2^1 2b_1^1$ orbital occupation. At the MRCI+D level the vertical excitation energy is 1.88 eV. The $^1A_1 \rightarrow {}^1A_2$ transition is symmetry-forbidden. At the optimized geometry of $^1A_2$ the C^1C^2 bond is elongated to 1.39 Å and the C^2C^3 bond only slightly lengthens. Both CASSCF and CIS calculations show that the C_{2v} symmetric structure of $^1A_2$ has no imaginary frequencies. The adiabatic excitation energies of $^1A_2$ is calculated to be 1.77 eV. The next state is $^1B_1$ ($1b_1^2 2b_1^1 7a_1^1 2b_2^2$) where one electron of the lone pair is shifted to the π^* orbital. At the optimized geometry, $^1B_1$ has a single C^1C^2 bond and a triple C^2C^3 bond with the π-components on the $1b_1$ and $2b_2$ orbitals. The unpaired electrons are located on C^1 ($2b_1$) and C^3 ($7a_1$). The vertical and adiabatic excitation energies of $^1B_1$ at the MRCI+D level are 2.44 and 2.05 eV, respectively, and the oscillator strength is 0.02. A recent study of Seburg et al.[44] showed that the vinylidenecarbene can undergo

TABLE 2: Relative Energies (kcal/mol) of Various Structures of Allene in the Ground and Excited Singlet Electronic States

	ZPE[a]	CASSCF(4,6)/6-311+G**	CASSCF(8,10)/ANO(2+)	MRCI(4,8)/ANO(2+)	MRCI+D/ANO(2+)
1, S_0, $^1A_1$ (D_{2d})[b]	34.4(0)	0.0	0.0	0.0	0.0
2a, S_0, ^1A_u (D_{2h})	33.5(3)	82.6	41.3	54.9	56.4
2b, S_1, ^1A_g (D_{2h})	32.7(1)	98.4	60.4	70.2	69.6
3, S_0, $^1A_2$ (C_{2v})	35.6(1)	76.3	25.6	46.7	48.8
4, S_0, $^1A_1$ (C_{2v})	34.5(1)	86.8	39.1	69.9	72.8
5, S_1, $^1A''$ (C_s)			45.4[c]	82.0[c]	70.3[c]
6, S_1, $^1A''$ (C_s)	33.7(1)	99.9			
7, S_2, $^1B_1$ (C_{2v})	39.0(0)	194.0	130.6	147.7	147.3
8, MSX (C_{2v}) $^1A_1$			38.9[c]	69.7[c]	72.5[c]
$^1A_2$			41.2[c]	64.5[c]	66.1[c]
9, MSX (D_{2h}) ^1A_g			156.7[c]	157.0[c]	147.4[c]
^1A_u			156.0[c]	161.1[c]	154.5[c]
10, S_1, $^1B_2$ (C_{2v}')	36.6(0)	137.1	94.2	110.8	108.3
11, S_3, $^1B_1$ (C_{2v}')	35.3(0)	146.2	149.4	169.3	158.6
TS2, S_1, $^1A''$ (C_s)			96.1[c]	134.6[c]	128.8[c]
$^1A'$			93.6[c]	133.4[c]	129.5[c]
TS1′, $^1A'$ (C_s)			100.4[c]	138.1[c]	135.2[c]
$^1A''$			104.1[c]	139.6[c]	133.8[c]

[a] Zero-point energies calculated at the CASSCF(4,6)/6-311+G** level. In parentheses: number of imaginary frequencies. [b] The total energies (in hartrees) for **1** are the following: CASSCF(4,6)/6-311+G**, −115.945 84; CASSCF(8,10)/ANO(2+), −115.967 84; MRCI(4,8)/ANO(2+), −116.333 56; MRCI+D/ANO(2+), −116.384 54. [c] Without ZPE corrections.

TABLE 3: Vertical and Adiabatic Excitation Energies (eV) for Vinylidenecarbene C_3H_2, Calculated at Various Levels of Theory

		ZPE[b]		CASSCF(8,10)	MRCI(4,8)	MRCI+D		EOM-CCSD	
state	character[a]	CAS[c]	CIS[d]	/ANO(2+)	/ANO(2+)	/ANO(2+)	osc str	/6-311(2+)G**	osc str
$^1A_1$[e]	ground state	19.4(0)		−114.747 98	−115.033 72	−115.075 94		−115.089 93	
$^1A_2$ vert	$\pi' \rightarrow \pi^*$			1.77	1.88	1.88	0.	1.97	0.
adiab		18.9(0)	19.8(0)	1.62	1.76	1.77			
$^1B_1$ vert	$n \rightarrow \pi^*$			2.61	2.73	2.44	0.016	2.80	0.010
adiab			20.9(0)	1.93	2.12	2.05			
2^1A_1 vert	$\pi \rightarrow \pi^* + \pi' \rightarrow \pi'^*$			6.01	5.57	5.39	0.075	5.62	0.166
adiab		19.0(0)	19.7(0)	5.24	5.12	4.92			
3^1A_1 vert	$\pi' \rightarrow \pi^*$ (2 e)			6.71	6.27	5.80	0.046	7.44	0.036
adiab			17.8(2)	6.00	5.75	5.43			
$^1B_2$ vert	$\pi' \rightarrow \pi^*$ & $n \rightarrow \pi^*$			6.58	5.92	5.84	0.0002	7.11	0.008
adiab			18.4(2)	6.19	5.80	5.82			
2^1A_2 vert	$\pi \rightarrow \pi^*$ & $\pi' \rightarrow \pi^*$			6.64	6.67	6.58	0.	7.80	0.
adiab	$\pi' \rightarrow 3p$		18.1(2)	6.04	5.88	5.81			

[a] See text for more detail. [b] Zero-point energies (kcal/mol). In parentheses: number of imaginary frequencies. [c] At the CASSCF(6,9)/6-311+G** level. [d] At the CIS/6-311+G** level. [e] For the ground state total energies are given in hartrees.

a photochemical automerization process at 444 nm. The electronic state which would absorb at this wavelength is $^1B_1$.

The next three singlet excited state lie significantly higher in energy than $^1A_2$ and $^1B_1$ but close to each other. The 2^1A_1 state has $\pi \rightarrow \pi^* + \pi' \rightarrow \pi'^*$ character and $1b_1^1 2b_1^1 7a_1^2 2b_2^1 3b_2^1$ dominant electronic configuration. The oscillator strength for the $^1A_1 \rightarrow 2^1A_1$ transition is relatively large. At the optimized geometry both CC bonds, especially C^2C^3, are stretched. Both CASSCF and CIS calculations give no imaginary frequencies for the C_{2v} structure of 2^1A_1. The energy of this state decreases from 5.39 eV at the ground state geometry to 4.92 eV at the optimized geometry. The third state in A_1 symmetry has the dominant electronic configuration of $1b_1^2 2b_1^2 7a_1^2 2b_2^0$, i.e., two electrons from the π' ($2b_2$) orbital are shifted to the π^* ($2b_1$) orbital. At the optimized geometry of 3^1A_1 C^1C^2 is a double bond, C^2C^3 is a single bond, and the electronic structure can be described as follows. The $1b_1$ orbital corresponds to the π-C^1C^2 bond, while C^3 has two lone pairs on the $7a_1$ and $2b_1$ orbitals. According to the significant geometry change, the difference between the vertical excitation energy (5.80 eV) and adiabatic excitation energy (5.43 eV) is substantial. CIS calculation gives two imaginary frequencies for 3^1A_1 indicating that the energy of the this state would further decrease upon CCC bending. The vertical energy of the $^1B_2$ state, 5.84 eV at the MRCI+D level, is close to that of 3^1A_1. The electronic configuration of $^1B_2$ is $1b_1^2 2b_1^2 7a_1^1 2b_2^1$, i.e., one electron from $7a_1$ and one electron from $2b_2$ are moved to the π^* $2b_1$ orbital. Despite that, the optimized geometry of $^1B_2$ and the ground state are similar. This fact can be explained by the electronic structure of $^1B_2$; it has a π-bond between C^1 and C^2 ($1b_1$) and a one-electron π'-bond between C^2 and C^3 ($2b_2$) and the $2b_1$ orbital contains a lone pair on the C^3 atom. The second unpaired electron is located on C^3 ($7a_1$). As a result of the small geometry change, the adiabatic excitation energy is only slightly lower than the vertical one. However, at the CIS level the C_{2v} structure of $^1B_2$ has two imaginary frequencies and the energy would decrease with symmetry distortion.

The sixth excited state is 2^1A_2, with the dominant electronic configurations of $1b_1^1 2b_1^2 7a_1^2 2b_2^1$ ($\pi \rightarrow \pi^*$ & $\pi' \rightarrow \pi^*$) and $1b_1^2 3b_1^1 7a_1^2 2b_2^1$ ($\pi' \rightarrow 3p$). At the optimized geometry within C_{2v} symmetry both CC bonds are elongated to 1.42−1.43 Å so that both π-bonds are broken. At the CIS level, the C_{2v} geometry of 2^1A_2 has two imaginary frequencies. The vertical and adiabatic (within C_{2v} symmetry) excitation energies of the 2^1A_2 state are 6.58 and 5.81 eV, respectively; however, the latter would decrease with the bending the CCC fragment.

Potential Energy Surfaces of H_2 Detachment from Allene. Profiles of the ground and excited state PES's for H_2 detachment are shown in Figure 4 and the energies of the reactants, products, and transition states are collected in Table 4. Figure 4 is a

TABLE 4: Relative Energies (kcal/mol, ZPE Corrections Are Included) of the Reactants, Products, and Transition States of the C_3H_4 (allene) → C_3H_2 + H_2 Reaction on the S_0 and T_1 Potential Energy Surfaces

	ZPE[a]	B3LYP/6-311G**	B3LYP/6-311+G**	CCSD(T)/6-311+G(3df,2p)	CCSD(T)/cc-pVTZ
C_3H_4, $^1A_1$, D_{2d}[b]	34.4(0)	−116.693 20	−116.695 27	−116.428 27	−116.433 31
C_3H_4, TS1, $^1A'$, C_s	28.0(1)	90.7		92.4	92.8
C_3H_2 ($^1A_1$,C_{2v}) + H_2	25.7(0)	84.8		83.0	83.8
C_3H_4, $^3A_2$, C_{2v}	32.7(0)		47.6	50.8	
C_3H_4, TS3, $^3A''$, C_s	25.3(1)		113.0	116.7	
C_3H_2 ($^3A''$,C_s) + H_2	24.2(0)	111.9	111.7	112.8	

[a] Zero-point energies calculated at the B3LYP/6-311G** level for singlets and at the B3LYP/6-311+G** level for triplets. In parentheses: number of imaginary frequencies. [b] The total energies (in hartrees).

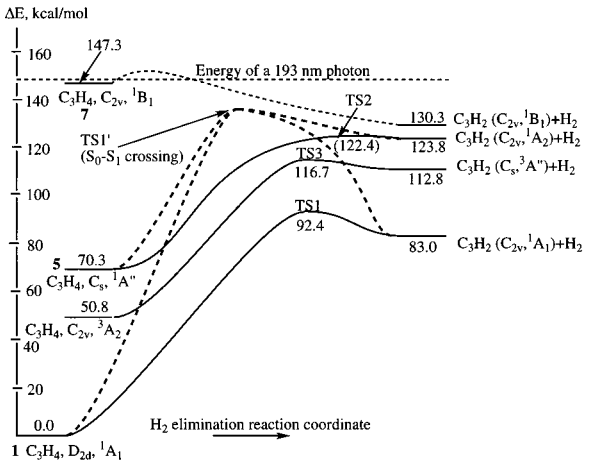

Figure 4. Schematic presentation of the profiles of potential energy surfaces along the reaction coordinate, corresponding to the H_2 elimination from allene, in various electronic states. The bold dashed curves illustrate the S_0-S_1 crossing in the vicinity of TS1′ and TS2. The dashed curve showing the S_2 surface is speculative.

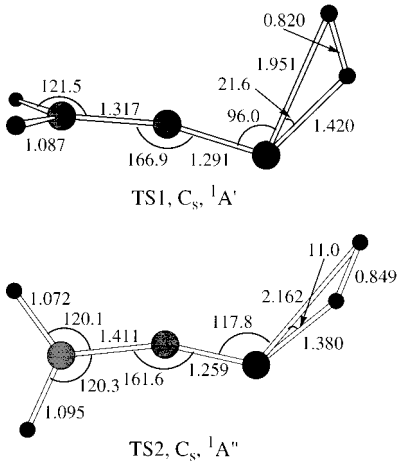

Figure 5. Optimized geometries of transition states for H_2 detachment from allene on the S_0 (B3LYP/6-311G**) and S_1 (s/a-CASSCF(8,10)/6-311+G**) PES.

schematic presentation of PES and the abscissa in this scheme is a reaction coordinate for H_2 elimination, which is not rigorously defined here. We only show the energies of the reactant, C_3H_4, the products, C_3H_2 + H_2, and the transition states in various electronic states. H_2 elimination from allene on the ground state surface occurs via transition state TS1, shown in Figure 5. The barrier is calculated to be 92.4 kcal/mol at the CCSD(T)/6-311+G(3df,2p) level with the B3LYP/6-311G(d,p) ZPE correction. The CCSD(T)/cc-pVTZ calculation gives a similar value for the barrier height. The calculated endothermicity of the C_3H_4 (allene) → C_3H_2 ($^1A_1$) + H_2 reaction is 83.0−83.8 kcal/mol. The experimental heats of formation for allene and C_3H_2 are 45.6 and 129.4 kcal/mol, respectively;[45] thus, the agreement between theory and experiment is close. The reverse barrier for H_2 addition to the vinylidenecarbene C_3H_2 is 9.0−9.4 kcal/mol. This value is close to the barrier height for H_2 addition to vinylidene to form C_2H_4, 12.2 kcal/mol at the MP4(SDQ)/6−31G** level.[46] TS1 is a late transition state for H_2 elimination. Geometries of the C_3H_2 and H_2 fragments in TS1 are close to those of the free molecules. The HH bond in H_2 is stretched only by 0.07 Å. The CCC fragment is slightly bent. The breaking CH bond distances are uneven, 1.42 and 1.95 Å.

According to the energy balance, C_3H_2 can be also produced in the first excited $^1A_2$ state. This state correlates to the first excited state of allene, structures **2b** (^1A_g) or **5** ($^1A''$). **2b** and **5** lie by about 70 kcal/mol higher than the ground state allene and the C_3H_2 ($^1A_2$) + H_2 products are by ∼124 kcal/mol higher in energy than C_3H_4 **1**. The transition state for H_2 detachment on the S_1 surface is TS2. TS2 has a planar geometry, the HH is 0.85 Å, about 0.1 Å longer than in the free H_2. Similar to TS1, the breaking CH bonds have significantly different lengths, 1.38 and 2.16 Å. The energy of TS2 relative to **1** at the MRCI+D level is 128.8 kcal/mol without ZPE correction. Assuming that the ZPE correction is the same as for TS1, one gets for TS2 an energy of 122.4 kcal/mol. This is slightly lower than the energy of C_3H_2 ($^1A_2$) + H_2. The result indicates that the reverse C_3H_2 ($^1A_2$) + H_2 → C_3H_4 (S_1) reaction proceeds with a low barrier or without a barrier.

The minimum on the S_1 surface has a planar geometry. Therefore, after the photoexcitation the allene molecule tends to become planar. Crossing between S_1 and S_0 and hopping onto the ground state surface also is likely to happen at a planar geometry. On the other hand, the geometry of TS1 on the S_0 surface is not planar; one of the CH_2 groups is twisted by 90°. The trajectory from the excited C_3H_4 to C_3H_2 + H_2 may not necessarily go via the transition state, because the available energy is much higher than the barrier. For example, let us consider a structure TS1′, which is similar to TS1 but has two CH_2 groups in the same plane. The energy of TS1′ for the $^1A'$ state is 135.2 kcal/mol at the MRCI+D level, i.e., below the photon energy. Another interesting observation is that the energies of S_0 and S_1 are very close to each other at the geometries of TS1′ and TS2. At TS1′, the energies of $^1A'$ and $^1A''$ are 135.2 and 133.8 kcal/mol, respectively. At TS2, at the MRCI+D/ANO(2+) level, $^1A''$ (128.8 kcal/mol) is slightly lower than $^1A'$ (129.5 kcal/mol), although at the CASSCF(8,-10) level $^1A''$ is the excited state. This means that in the vicinity of TS1′ and TS2 the S_0 and S_1 surfaces cross, which is illustrated by the bold dashed curves in Figure 4. Note, this crossing occurs at the geometry quite different from those explored in Figure 2. Thus, one of the likely reaction scenarios is traveling along the S_1 surface from the ground state geometry to the vicinity of TS1′ and TS2 followed by hopping onto S_0 and elimination of H_2.

The second excited state of C_3H_2 ($^1B_1$), which also can be energetically accessed, correlates with C_3H_4 ($^1B_1$) **7** on the S_2 surface. The **7** → C_3H_2 ($^1B_1$) + H_2 reaction is exothermic, with

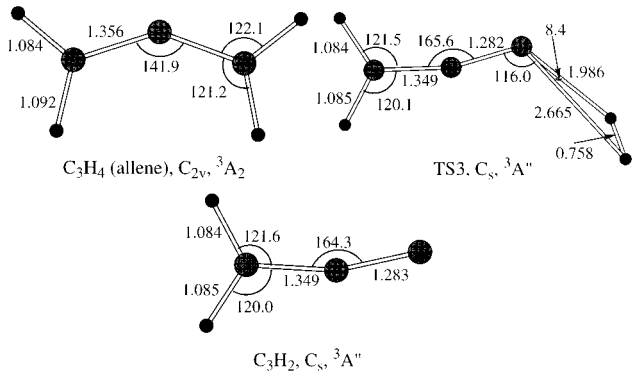

Figure 6. Optimized geometries (B3LYP/6-311+G**) of the reactant, product and transition state of the C_3H_4 (allene) → C_3H_2 + H_2 reaction on the triplet T_1 PES.

the energy release of ~17 kcal/mol. **7** is a local minimum on the S_2 surface, therefore, it is separated from C_3H_2 ($^1B_1$) + H_2 by a barrier. Since the energy of **7** is 147.3 kcal/mol relative to **1**, even a very low barrier would bring the energy higher than the energy available from the 193 nm photoexcitation, as shown by the dashed curve in Figure 4. Hence, the formation of C_3H_2 in the $^1B_1$ state from the photodissociation of allene at this wavelength is unlikely.

On account of the possibility that the H_2 detachment could occur on the triplet surface after the photoexcitation followed by the intersystem crossing, we also considered the reactant, transition state, and products on T_1 PES. Their B3LYP optimized geometries are shown in Figure 6. The triplet allene ($^3A_2$) has a planar C_{2v} symmetric structure which is similar to that of **3** ($^1A_2$). Opposite to **3**, the triplet structure has no imaginary frequencies and is a local minimum on T_1. The adiabatic singlet−triplet separation for allene is calculated to be 50.8 kcal/mol at the CCSD(T)/6-311+G(3df,2p) level with B3LYP/6-311G(d,p) ZPE corrections. The energy of C_3H_4 ($^3A_2$) is close to the energy of **3** ($^1A_2$), indicating that the T_1 and S_0 surfaces may cross in this vicinity. For C_3H_2, the lowest vertical triplet state is also $^3A_2$, however, optimization leads to the distortion of symmetry from C_{2v} to C_s. At the optimized structure the electronic term is $^3A''$. The CCC angle changes from linear to 164.3°. The CC distances are somewhat shorter than those in C_3H_2 ($^1A_2$). The adiabatic singlet−triplet gap for vinylidenecarbene is 29.8 kcal/mol, which agrees with the results of previous calculations[47] and the experimental value of 29.7 ± 0.2 kcal/mol.[45] The C_3H_2 ($^3A''$) + H_2 products lie by 112.8 kcal/mol higher than the ground state allene **1**. The transition state for H_2 elimination on the T_1 surface, TS3, has a very late character; the HH bond is only 0.01 Å longer than that in H_2 and the shortest breaking CH bond distance is 1.99 Å. The energy of TS3 is 116.7 kcal/mol at the CCSD(T) level with ZPE, and the reverse barrier on the T_1 surface is about 4 kcal/mol.

Applications to the Photodissociation Dynamics. The most likely mechanism of the photodissociation of allene at 193 nm involves as the initial step vertical excitation to the $^1B_1$ state,

$$CH_2CCH_2\ (S_0,{}^1A_1) + h\nu_{193\ nm} \rightarrow CH_2CCH_2\ (S_2,{}^1B_1)$$

The difference between the energy of a photon and the adiabatic excitation energy for the corresponding equilibrium structure **2b** on the excited state PES is very large, ~78 kcal/mol. Therefore, the molecule formed in the excited electronic state should also be highly vibrationally excited,

$$CH_2CCH_2\ (S_2,{}^1B_1) \rightarrow C_3H_4^{\ddagger}\ \mathbf{2b}\ (S_1,{}^1A_g)$$

Particularly, since the molecule in the excited state tends to become planar, the normal mode corresponding to the internal CH_2 rotation should be excited. On the next stage, conversion into the vibrationally excited ground electronic state takes place by hopping from S_1 to S_0 on the seam of their crossing,

$$C_3H_4\ (S_1) \rightarrow C_3H_4^{\ddagger}\ (S_0)$$

This can happen at the planar C_{2v} symmetric geometries, between structures **8** and **9**, and would lead to vibrational excitation of the CC stretching and CCC and CCH bending modes in the ground state. On the other hand, the hopping can occur along the pathway of H_2 detachment in the vicinity of TS2 and TS1′.

The last reaction step is elimination of H_2 on the ground state surface,

$$C_3H_4^{\ddagger}\ (S_0) \rightarrow C_3H_2\ (^1A_1) + H_2$$

According to the experimental $P(E_T)$ curve for this reaction,[1] the translational energy of the products lies in the 6−34 kcal/mol range. If C_3H_2 is formed in the excited $^1A_2$ and $^1B_1$ electronic states, ΔH is 124 and 130 kcal/mol and the total energy disposal, $h\nu - \Delta H$, is 24 and 18 kcal/mol, respectively, significantly lower than the observed maximal threshold of E_T. If C_3H_2 is formed in the triplet $^3A''$ state, the energy disposal, ~35 kcal/mol, is close to the maximal threshold of $P(E_T)$, however, the triplet scenario can be achieved only via intersystem crossing and is expected to be less likely.

The experimental minimal threshold of E_T approximately corresponds to the reverse barrier (~9 kcal/mol) on the ground state PES. This is reasonable because at the transition state geometry (TS1), C_3H_2 and H_2 are only slightly distorted and their internal energy is small (2−3 kcal/mol). After TS1 the reaction occurs fast and all or most of the potential energy should be transformed into the translational energy. If the dissociation takes place along the S_1 and T_1 surfaces, the $P(E_T)$ curve would have a zero or low minimal energy threshold, which is not the case in experiment.

Hence, we conclude that the C_3H_2 + H_2 products are formed in the ground state, ΔH is 83 kcal/mol, and the total energy disposal is 65 kcal/mol. This means that the internal energy of C_3H_2 + H_2 should be in the 31−59 kcal/mol range. The internal energy includes the following components,

$$E_{Int} = E_{vib}(H_2) + E_{rot}(H_2) + E_{vib}(C_3H_2) + E_{rot}(C_3H_2)$$

Here, the rotational energies of the fragments are related by conservation of the angular momentum. The distribution of energy among E_T and the components of the internal energy is determined by the photodissociation dynamics, i.e., by the trajectories the molecule travels along the excited and ground state PES. Also, it is important what is the first point on the seam of crossing the molecule reaches and what is the shape of the seam of crossing.

The mechanism discussed here implies that the products can be rotationally excited. This can be due to the excitation of the normal mode corresponding to the CH_2 internal rotation, leading to the pinwheel rotation of H_2 and the rotation of C_3H_2 around the CCC axis. This kind of C_3H_2 rotation does not cause the rotational excitation of C_3 after the second H_2 detachment. In the transition state TS1 one H is much closer to the carbon center than the other. The C−H repulsion for the close H atom is much greater than for the other H atom and therefore some torque is exerted on the H_2 species. This results in the cartwheel rotational excitation of H_2. Experimental measurements of

Stolow et al.[48] who have studied the photodetachment of H_2 from ethylene and allene showed that J number for H_2 molecules can be as high as 11, which corresponds to an energy of 23 kcal/mol. On the other hand, the most probable value of $J(H_2)$ is 3; E_{rot} $(H_2) = 2.1$ kcal/mol. This must correspond to the most probable value of the translational and vibrational energy, $E_T = 20$ kcal/mol and $E_{vib}(H_2) = 0$, because most H_2 is formed with $v = 0$. Therefore, $E_{rot}(C_3H_2) + E_{vib}(C_3H_2) = \sim 43$ kcal/mol. The rotational energy of C_3H_2 cannot be higher 1−2 kcal/mol owing to conservation of angular momentum. Thus, the most probable value of $E_{vib}(C_3H_2)$ is about 40 kcal/mol. Calculating the energies of the C_3H_2 fragments in structures **8** and **9** on the seam of crossing relative to the free C_3H_2, we get 33 and 63 kcal/mol, respectively. Therefore, it is likely that the C_3H_2 product bears the internal energy of the C_3H_2 fragment if the dissociation on the ground state PES is fast after the S_1-S_0 hopping occurs.

Concluding Remarks

Three singlet excited electronic states of allene, $^1A_2$, $^1B_1$, and ^1E, could absorb 193-nm photons and their respective vertical excitation energies are calculated to be 6.10, 6.55 and 6.94 eV. Three local minima are found on the S_1 surface, **2b** (^1A_g, D_{2h}), **5** ($^1A''$, C_s) and **10** ($^1B_2$, C_{2v}'), and their adiabatic excitation energies are 3.02, 3.05, and 4.70 eV, respectively. On the S_2 and S_3 PES's the minima are **7** ($^1B_1$, C_{2v}) and **11** ($^1B_1$, C_{2v}') with the energies of 6.39 and 6.88 eV. The geometry changes in the excited states of allene are very large compared to the geometry of the ground state. The potential energy surfaces of the ground and excited states cross when geometry of the molecule changes by twisting the CH_2 groups and bending the CCC angle or along the pathway that leads to H_2 detachment.

For vinylidenecarbene C_3H_2, the lowest lying singlet excited states are $^1A_2$ (1.88 eV) and $^1B_1$ (2.44 eV), and the next three states, 2^1A_1, 3^1A_1, and $^1B_2$, have vertical excitation energies in the 5.39−5.84 eV range. Geometries of the first three excited states remain C_{2v} symmetric, and only CC bond lengths change as compared to the ground state geometry.

The most likely mechanism for photodissociation of allene at 193 nm to produce $C_3H_2 + H_2$ involves a Franck−Condon transition to the $^1B_1$ excited state. This is followed by a twisting of the CH_2 groups and then conversion to the vibrationally excited ground state through the seam of crossing. Once the vibrationally excited allene molecule is in the ground electronic state it dissociates to produce $C_3H_2 + H_2$. According to the experimental $P(E_T)$ curve and our calculations, the $C_3H_2 + H_2$ products formed in the ground state should have at least ∼31 kcal/mol of internal energy. A significant fraction of the internal energy is speculated to be due to the vibrational excitation of C_3H_2 and the rotational excitation of H_2. A more detailed understanding of the $P(E_T)$ curve and the distribution between the translational and internal (vibrational and rotational) energies of the products requires the determination of the ground and excited states potential energy surfaces over the full range of configuration space explored in the dissociation, the determination of the crucial nonadiabatic matrix elements which govern the surface crossings, and, finally, the simulation of dynamics of the nonadiabatic dissociation.

Acknowledgment. A.M.M. is grateful to Academia Sinica for his fellowship at IAMS. This work supported in part by the National Science Council of ROC. W.M.J. gratefully acknowledges the support of IAMS for his visiting Professorship position and NASA under Grant NAGW-5083.

References and Notes

(1) Jackson, W. M.; Anex, D. S.; Continetti, R. E.; Lee, Y. T. *J. Phys. Chem.* **1991**, *95*, 7327.
(2) Song, X.; Bao, Y.; Urdahl, R. S.; Gosine, J. N.; Jackson, W. M. *Chem. Phys. Lett.* **1994**, *217*, 216.
(3) Jackson, W. M. In *Comets in the Post-Halley Era*; Newburn, R. L., Ed.; Kluwer Academic Publishers: Amsterdam, 1991; Vol. 1, p 313.
(4) Slagle, I. R.; Gutman, D. In *Twenty-First Symposium (Interanational) on Combustion*, The Combustion Institute: Pittsburgh, PA, 1986, p 875.
(5) Thaddeus, P.; Vrtilek, J. M.; Gottlieb, C. A. *Astrophys. J.* **1985**, *299*, L63.
(6) Marsden, B. G. *Annu. Rev. Astron. Astrophys.* **1974**, *12*, 1.
(7) Jackson, W. M. In *Laboratory studies of photochemical and spectroscopic phenomena related to comets*, Wilkening, L. L., Ed.; University of Arizona: Tempe, AZ, 1982; p 480.
(8) Honjou, N.; Pacansky, J.; Yoshimine, M. *J. Am. Chem. Soc.* **1985**, *107*, 5322.
(9) Yoshimine, M.; Pacansky, J.; Honjou, N. *J. Am. Chem. Soc.* **1989**, *111*, 2785.
(10) Yoshimine, M.; Pacansky, J.; Honjou, N. *J. Am. Chem. Soc.* **1989**, *111*, 4198.
(11) Honjou, N.; Yoshimine, M.; Pacansky, J. *J. Phys. Chem.* **1987**, *91*, 4455.
(12) (a) Becke, A. D. *J. Chem. Phys.* **1993**, *98*, 5648; (b) *Ibid.* **1992**, *96*, 2155; (c) *Ibid.* **1992**, *97*, 9173. (d) Lee, C.; Yang, W.; Parr, R. G. *Phys. Rev.* **1988**, *B37*, 785.
(13) For the description of basis sets of the 6-311G(d,p) type, see: Hehre, W. J.; Radom, L.; Schleyer, P. v. R.; Pople, J. *Ab Initio Molecular Orbital Theory*; Wiley: New York, 1986.
(14) (a) Purvis, G. D.; Bartlett, R. J. *J. Chem. Phys.* **1982**, *76*, 1910. (b) Scuseria, G. E.; Janssen, C. L.; Schaefer, H. F., III *J. Chem. Phys.* **1988**, *89*, 7382; (c) Scuseria, G. E.; Schaefer, H. F., III *J. Chem. Phys.* **1989**, *90*, 3700. (d) Pople, J. A.; Head-Gordon, M.; Raghavachari, K. *J. Chem. Phys.* **1987**, *87*, 5968.
(15) (a) Bauschlicher, C. W., Jr.; Partridge, H. *J. Chem. Phys.* **1995**, *103*, 1788. (b) Bauschlicher, C. W., Jr.; Partridge, H. *Chem. Phys. Lett.* **1995**, *240*, 533.
(16) (a) Mebel, A. M.; Morokuma, K.; Lin, M. C. *J. Chem. Phys.* **1995**, *103*, 7414. (b) Mebel, A. M.; Morokuma, K.; Lin, M. C.; Melius, C. F. *J. Phys. Chem.* **1995**, *99*, 1900. (c) Mebel, A. M.; Morokuma, K.; Lin, M. C. *J. Chem. Phys.* **1995**, *103*, 3440;
(17) Dunning, T. H. *J. Chem. Phys.* **1989**, *90*, 1007.
(18) (a) Schlegel, H. B.; Robb, M. A. *Chem. Phys. Lett.* **1982**, *93*, 43; (b) Bernardi, F.; Bottoni, A.; McDougall, J. J. W.; Robb, M. A.; Schlegel, H. B. *Faraday Symp. Chem. Soc.* **1984**, *19*, 137.
(19) (a) Werner, H.-J.; Knowles, P. J . *J. Chem. Phys.* **1985**, *82*, 5053. (b) Knowles, P. J.; Werner, H.-J. *Chem. Phys. Lett.* **1985**, *115*, 259.
(20) Foresman, J. B.; Head-Gordon, M.; Pople, J. A.; Frisch, M. J. *J. Phys. Chem.* **1992**, *96*, 135.
(21) (a) Werner, H.-J.; Knowles, P. J. *J. Chem. Phys.* **1988**, *89*, 5803. (b) Knowles, P. J.; Werner, H.-J. *Chem. Phys. Lett.* **1988**, *145*, 514.
(22) Widmark, P.-O.; Malmqvist, P.-Å.; Roos, B. O. *Theor. Chim. Acta* **1990**, *77*, 291.
(23) Serrano-Andres, L.; Merchan, M.; Nebot-Gil, I.; Lindh, R.; Roos, B. O. *J. Chem. Phys.* **1993**, *98*, 3151.
(24) Stanton, J. F.; Bartlett, R. J. *J. Chem. Phys.* **1993**, *98*, 7029.
(25) Wiberg, K. B.; Hadad, C. M.; Foresman, J. B.; Chupka, W. A. *J. Phys. Chem.* **1992**, *96*, 10756.
(26) MOLPRO is a package of *ab initio* programs written by H.-J. Werner and P. J. Knowles, with contributions from J. Almlöf, R. D. Amos, M. J. O. Deegan, S. T. Elbert, C. Hampel, W. Meyer, K. Peterson, R. Pitzer, A. J. Stone, P. R. Taylor, and R. Lindh.
(27) Frisch, M. J.; Trucks, G. W.; Schlegel, H. B.; Gill, P. M. W.; Johnson, B. G.; Robb, M. A.; Cheeseman, J. R.; Keith, T.; Petersson, G. A.; Montgomery, J. A.; Raghavachari, K.; Al-Laham, M. A.; Zakrzewski, V. G.; Ortiz, J. V.; Foresman, J. B.; Cioslowski, J.; Stefanov, B. B.; Nanayakkara, A.; Challacombe, M.; Peng, C. Y.; Ayala, P. Y.; Chen, W.; Wong, M. W.; Andres, J. L.; Replogle, E. S.; Gomperts, R.; Martin, R. L.; Fox, D. J.; Binkley, J. S.; Defrees, D. J.; Baker, J.; Stewart, J. P.; Head-Gordon, M.; Gonzalez, C.; Pople, J. A. GAUSSIAN 94, Revision B.2; Gaussian, Inc.; Pittsburgh: PA, 1995.
(28) Stanton, J. F.; Gauss, J.; Watts, J. D.; Lauderdale, W. J.; Bartlett, R. J. ACES-II, University of Florida.
(29) Fuke, K.; Schnepp, O. *Chem. Phys.* **1979**, *38*, 211.
(30) Rabalais, J. W.; McDonald, J. M.; Scherr, V.; McGlynn, S. P. *Chem . Rev.* **1971**, *71*, 73.
(31) Iverson, A. A.; Russell, B. R. *Spectrochim. Acta, Part A* **1972**, *28*, 447.
(32) Robin, M. B. In *Higher Excited States of Polyatomic Molecules*, Vol. 2; Academic Press: New York, 1975; Vol. 2.
(33) Rauk, A.; Drake, A. F.; Mason, S. F. *J. Am. Chem. Soc.* **1979**, *101*, 2284.
(34) Diamond, J.; Segal, G. A. *J. Am. Chem. Soc.* **1984**, *106*, 952.

(35) Galasso, V.; Fronzoni, G. *J. Mol. Struct. (THEOCHEM)* **1985**, *133*, 235.
(36) Seeger, R.; Krishnan, R.; Pople, J. A.; Schleyer, P. v. R. *J. Am. Chem. Soc.* **1977**, *99*, 7103.
(37) Martin, P. S.; Yates, K.; Csizmadia, I. G. *J. Mol. Struct. (THEOCHEM)* **1988**, *170*, 107.
(38) (a) Valtazanos, P.; Elbert, S. T.; Xantheas, S.; Ruedenberg, K. *Theor. Chim. Acta* **1991**, *78*, 287. (b) Xantheas, S.; Elbert, S. T.; Ruedenberg, K. *Theor. Chim. Acta* **1991**, *78*, 365.
(39) Bettinger, H. F.; Schreiner, P. R.; Schleyer, P. v. R.; Schaefer, III, H. F. *J. Phys. Chem.* **1996**, *100*, 16147.
(40) Roth, W. R.; Ruf, G.; Ford, P. W. *Chem. Ber.* **1974**, *107*, 48.
(41) Lam, B.; Johnson, R. P. *J. Am. Chem. Soc.* **1983**, *105*, 7479.
(42) Buenker, R. J.; Peyerimhoff, S. D. *Chem. Rev.* **1974**, *74*, 127.
(43) (a) Mebel, A. M.; Chen, Y. T.; Lin, S. H. *Chem. Phys. Lett.* **1996**, *258*, 53. (b) Mebel, A. M.; Chen, Y. T.; Lin, S. H. *J. Chem. Phys.* **1996**, *105*, 9007.
(44) Seburg, R. A.; Patterson, E. V.; Stanton, J. F.; McMahon, R. J. *J. Am. Chem. Soc.* **1997**, *119*, 5847.
(45) Robinson, M. S.; Polak, M. L.; Bierbaum, V. M.; DePuy, C. H.; Lineberger, W. C. *J. Am. Chem. Soc.* **1995**, *117*, 6766.
(46) Raghavachari, K.; Frisch, M. J.; Pople, J. A.; Schleyer, P. v. R. *Chem. Phys. Lett.* **1982**, *85*, 145.
(47) Jonas, V.; Böhme, M.; Frenking, G. *J. Phys. Chem.* **1992**, *96*, 1640.
(48) (a) Cromwell, E. F.; Stolow, A.; Vrakking, J. J.; Lee, Y. T. *J. Chem. Phys.* **1992**, *97*, 4029. (b) Stolow, A., private communications.